Article

JOURNAL OF
biomaterials
applications

Journal of Biomaterials Applications
2022, Vol. 0(0) 1–9

DOI: 10.1177/08853282221114450
journals.sagepub.com/home/jba
SAGE

Guided bone regeneration with extracellular matrix scaffold of small intestinal submucosa membrane

Zihao Liu[1,†], Pengfei Wei[2,†], Qingying Cui[3,†], Yuzhu Mu[4], Yifan Zhao[4], Jiayin Deng[4], Min Zhi[4], Yi Wu[4], Wei Jing[2], Xian Liu[5], Jihong Zhao[6] and Bo Zhao[2]

Abstract

Guided bone regeneration (GBR) is a promising strategy for repairing bone defects using bioactive membranes. In this study, a new type of GBR membrane based on the small intestinal submucosa (SIS) was created, and its surface structure, cytological characteristics, and bone defect repair ability were compared with commonly used membranes. Our results show that compared to the Heal-all and Dentium membranes, the SIS membrane has an asymmetric structure that does not affect the proliferation of bone marrow mesenchymal stem cells (BMSCs). Instead, it increased their formation of calcium nodules and expression of bone morphogenetic protein-2 (BMP-2), alkaline phosphatase (ALP), runt-related transcription factor 2 (Runx2), and osteopontin (OPN). Six weeks after their insertion into a rat calvarial defect model, increased bone growth was observed in the SIS membrane group. Our results indicate that the SIS membrane has good biocompatibility and is more effective in promoting early bone formation than existing membranes. Given the wide range of source materials and simple preparation processes available, SIS membrane is a promising candidate for guided bone regeneration.

Keywords

Bone defect, guided bone regeneration, small intestinal submucosa, absorbable membrane, osteogenesis

Introduction

Bone defects are a common issue in clinical practice.[1,2] In recent years, guided bone regeneration (GBR) technologies have provided a new treatment option for bone defect repair and other oral clinical issues such as alveolar bone loss and deficiency caused by periodontitis and tooth loss.[3,4]

Guided bone regeneration treatments use a barrier membrane to prevent the growth of fibroblasts from surrounding soft tissues, providing osteoblasts at the bone's surface sufficient time to proliferate and complete tissue regeneration and directional repair.[5] GBR membranes can be divided into two types based on their degradation characteristics: non-absorbable and absorbable.[6] The primary component of non-absorbable membranes is polytetrafluoroethylene, the earliest membrane material used in clinical applications.[6] However, it must be surgically removed after treatment is completed, increasing patients' pain, discomfort, and economic burden.[7] Absorbable membranes, such as collagen and polymer membranes, have been developed to overcome this issue and have become the preferred option in clinical applications.[8,9]

Collagen is the primary component of animal skin, bone, and connective tissue, making it a suitable scaffold material in tissue engineering.[10] Because of its excellent biocompatibility and degradability, collagen membranes are the most widely used for guided tissue regeneration in clinical

[1]Tianjin Nankai Zhongnuo Stomatological Hospital, Tianjin, China
[2]Beijing Biosis Healing Biological Technology Co, Ltd, Beijing, China
[3]School of Stomatology Kunming Medical University, Kunming, China
[4]School and Hospital of Stomatology, Tianjin Medical University, Tianjin, China
[5]State Key Laboratory of Oral Diseases, West China Hospital of Stomatology, Sichuan University, ChengDu, China
[6]The State Key Laboratory Breeding Base of Basic Science of Stomatology (Hubei-MOST) & Key Laboratory of Oral Biomedicine Ministry of Education, School &Hospital of Stomatology, Wuhan University, Wuhan, China

[†]ZL, PW and QC contributed equally to this work

Corresponding author:
Zihao Liu, Tianjin Nankai Zhongnuo Stomatological Hospital, Dingfu building at the Intersection of Nankai Third Road and Nanma Road, Tianjin 300100, China.
Email: liuzihao@tmu.edu.cn

applications.[11] In recent years, many collagen membranes have been developed and used as a barrier to promote bone regeneration in the GBR field with good results, including Heal-all and Dentium. However, new GBR membranes containing bioactive substances that improve their regeneration and barrier functions have the potential to improve the clinical efficacy of GBR surgery.

In recent years, the extracellular matrix (ECM) has been found to play a positive role in tissue regeneration through its regulatory effects on cell proliferation, survival, migration, and differentiation, which help maintain tissue homeostasis and repair.[12–14] The small intestinal submucosa (SIS) is a type of acellular, natural collagen ECM composed primarily of type I and type III collagen and small amounts of type V and type VI collagen. It has site-specific tissue regeneration abilities and excellent mechanical properties and can be used as a substitute for tissue engineering, which hardly cause immune rejection.[15] In addition, SIS contains glycosaminoglycan, fibronectin, chondroitin sulfate, heparin, and various cytokines, including fibroblast growth factor (FGF), epidermal growth factor (EGF), transforming growth factor (TGF), and vascular endothelial growth factor (VEGF).[16,17] While playing a supporting role, SIS can help regulate cellular activities and promote tissue repair and regeneration.[18] It has been used as a tissue engineering skeleton material in numerous fields, including bone and cartilage, skin, and tympanic membrane repair.[19–21] Therefore, SIS has great potential in GBR.

This study used in vitro and in vivo experiments to explore the surface characteristics, biocompatibility, and bone regeneration ability of SIS membrane materials, and provides new opportunities for barrier membrane development in GBR surgery.

Materials and methods

Preparation of SIS membrane

The SIS membrane used in this study was obtained from Beijing Biosis Healing Biological Technology Co, Ltd (Beijing, China) and derived from the submucosa of the pig small intestine. Its preparation process is described as follows: First, the small intestines were mechanically removed the tunica mucosa, the entire tunica muscularis externa and the serosa, and then washed with phosphate-buffered saline (PBS; Solarbio; Beijing, China). Secondly, the prepared SIS was soaked into peroxyacetic acid and ethanol for 30 min and rinsed with saline solution. Thirdly, the material was incubated in the trypsin/EDTA (Gibco; Waltham, MA, USA) and rinsed with a saline solution. The multi-layer composited samples were lyophilized and sterilized using ethylene oxide (EO) gas. The Heal-all and Dentium membranes used in this study were derived from cattle.

Surface morphology of SIS membrane

Membrane morphology was observed by scanning electron microscopy (SEM) with an operating voltage of 10 kV after sputter-coating with gold (Nova NanoSEM430, Netherland).

In vitro cell culture

A cell culture plate without a membrane was used as the control group. The Heal-all membrane, Dentium membrane, or SIS membrane was placed onto the culture plate and used as the experimental group. Rat bone marrow mesenchymal stem cells (BMSCs; Cyagen Biosciences; Jiangsu, China) were grown in Dulbecco's modified Eagle's medium (DMEM; Gibco) with 10% fetal bovine serum (FBS; Gibco), 100 U/mL penicillin G (Gibco), and 100 mg/mL streptomycin (Gibco) at 5% CO_2 and 37°C. After 3 days, the culture medium was replaced by the osteoinductive medium that contained 100 nM dexamethasone, 50 μM ascorbate, and 10 mM β-glycerophosphate (Sigma-Aldrich; Burlington, MA, USA).

Cell proliferation assay

Cell proliferation was evaluated using a Cell-Counting Kit-8 (CCK8; Solarbio). After BMSCs were incubated in a 5% CO_2 incubator at 37°C for 4 h, the optical density (OD) value at 450 nm was obtained.

Alizarin red staining

The three membrane materials were immersed in DMEM medium for 3 days to obtain a corresponding leaching solution. BMSCs were inoculated on the cell crawling in 24-well plates incubated with the leaching solution for 3 days and then replaced with the osteoinductive medium prepared from the leaching solution. After 7 days, the cell crawling was fixed with 4% paraformaldehyde (Solarbio) for 30 min. After cleaning with PBS (Solarbio) three times, an appropriate amount of alizarin red dye was added to the sample (Solarbio) for 3–5 min before visualization and image capture under an inverted microscope (Olympus; Tokyo, Japan) after sealing.

Quantitative real-time polymerase chain reaction analysis

After culturing for 5 and 7 days, total BMSC RNA was extracted using TRIzol Reagent (Invitrogen; Carlsbad, CA, USA), and reverse transcription was performed using EasyScript One-Step gDNA Removal and cDNA Synthesis SuperMix (TransGen Biotech; Beijing, China). The mRNA expression level of bone morphogenetic protein-2 (*Bmp-2*),

runt-related transcription factor 2 (*Runx2*), alkaline phosphatase (*Alp*), and osteopontin (*Opn*) was determined with PerfectStart Green qPCR SuperMix (TransGen Biotech) using glyceraldehyde 3-phosphate dehydrogenase (*Gapdh*) as the standardization control and the primers listed in Table 1. The fold difference of each gene was calculated with the $^{\Delta\Delta}$Ct method.

Western blot analysis

After BMSC culturing, proteins were separated by electrophoresis and transferred to polyvinylidene fluoride (PVDF) membranes (Sigma-Aldrich). PVDF membranes were then blocked for 1 h with 5% bovine serum albumin (BSA; Solarbio) at room temperature before incubation with BMP-2, Runx2, ALP, and OPN primary antibodies (Abcam; Cambridge, UK) at 4°C overnight. Membranes were then incubated with a secondary antibody (Abcam) at room temperature for 1 h. All expression values were normalized to GAPDH.

Cellular immunofluorescence assays and confocal imaging

After culturing, BMSCs were fixed with 4% formaldehyde (Solarbio; Beijing, China) at room temperature for 20 min and permeabilized with 0.25% TritonX-100 (Sigma-Aldrich) for 5 min. Next, we immunostained for BMP-2, Runx2, ALP, and OPN using the corresponding antibody (Abcam) at 4°C overnight. A secondary antibody (Abcam) conjugated with fluorescein isothiocyanate (FITC; green) was then used to label cells for 1 h. DAPI (4′,6-diamidino-2phenylindole, blue, Solarbio) was used to stain the cell nuclei. Cells were imaged with a confocal laser scanning microscope (CLSM; Nikon Air Confocal; Rhodes, NSW, Australia).

Animal experiments

All animal experiments were approved by the Animal Ethical Committee of the Academic Medical Center at the Tianjin Medical University (Tianjin, China). Six to eight-week-old male Sprague-Dawley (SD) rats were randomly divided into the blank, Heal-all membrane, Dentium membrane, and SIS membrane groups, at least three in each group. An 8 mm critical bone defect was prepared on the rat skull using a ring drill. In this process, normal saline was used for flushing to reduce the temperature. Then, the membrane material was implanted in the defect, and the incision was sutured.

Analysis of bone regeneration in vivo

Skull specimens were collected 6 weeks post-operation. The bone regeneration in the skull defect area was evaluated by micro-CT analysis (SkyScan 1276; Bruker; Karlsruhe, Germany). Three-dimensional (3D) image reconstruction was performed with CTAn Software (Bruker), and bone-volume/total-volume (BV/TV) was calculated. The specimens were then decalcified for 30 days. After dehydration, tissues were embedded in paraffin and cut into 5 μm thick sections before hematoxylin−eosin (H&E; Solarbio) and Masson's trichrome (Solarbio) staining for histological analysis.

Table 1. RT-qPCR primer sequences.

Gene	Primer sequences (5′–3′)
Bmp-2	F: TGCGGTCTCCTAAAGGTCG R: ACTCAAACTCGCTGAGGACG
Runx2	F: CCGAACTGGTCCGCACCGAC R: CTTGAAGGCCACGGGCAGGG
Alp	F: TGACCACCACTCGGGTGAA R: GCATCTCATTGTCCGAGTACCA
Opn	F: GTGGTGATCTAGTGGTGCCAAGAGT R: AGGCACCGGCCATGTGGCTAT
Gapdh	F: GACGGCCGCATCTTCTTGTGC R: TGCAAATGGCAGCCCTGGTGA

Statistical analysis

All results are presented as mean ± standard deviation (SD) in each group. They were analyzed by single-factor analysis of variance (ANOVA) with Tukey's Test. A p-value <0.05 was considered statistically significant.

Results

Morphological observation

The surface morphologies of the three materials were observed by SEM. The right and back surfaces of the Heal-all membrane were found to have the same dense structure, with thicker and more obvious fibers (Figure 1a). The Dentium membrane was similar to the Heal-all membrane, but its fiber structure was finer (Figure 1b). In comparison, the SIS membrane was asymmetric with a dense and flat front and loose and porous back (Figure 1c).

Cell proliferation

After culturing for 1, 3, 5, and 7 days, the proliferation of BMSCs on each of the three membranes and in the blank control plate was assessed with CCK8. It found the density of cells in all groups to increase over time (Figure 2), indicating that the three membrane materials had no apparent cytotoxicity and satisfactory biocompatibility.

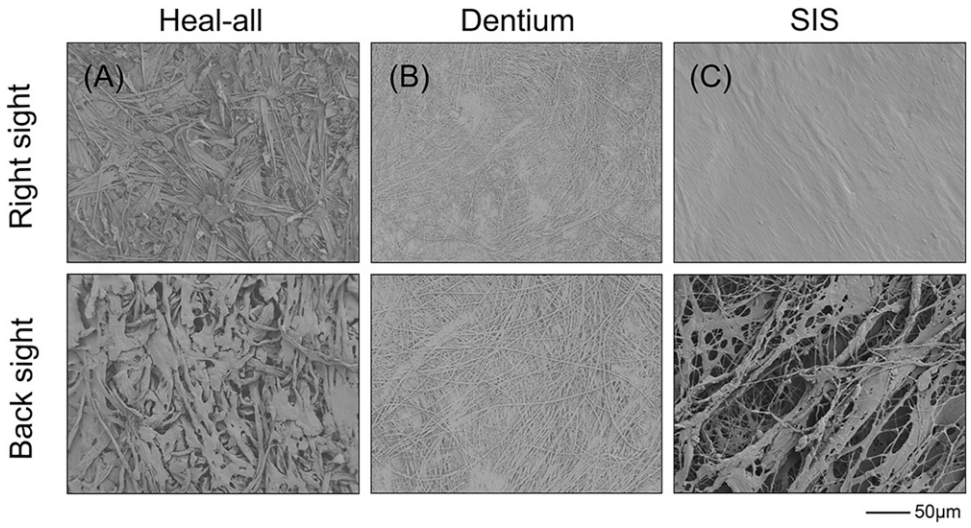

Figure 1. SEM images of Heal-all, Dentium, and SIS membranes. (a) Heal-all membrane. (b) Dentium membrane. (c) SIS membrane. All images were taken at 2000×.

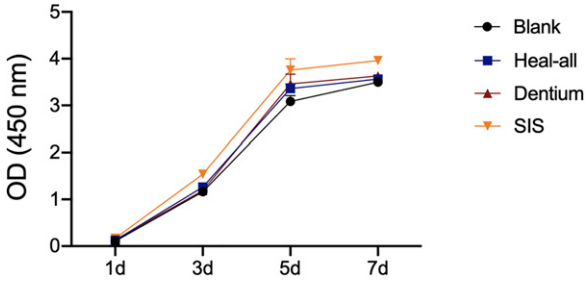

Figure 2. The proliferation of BMSCs cultured with each membrane.

Mineralized nodule staining

We explored the osteogenic differentiation of BMSCs on each membrane material after 7 days of culturing by observing their calcium deposition with alizarin red staining. We observed more red calcium nodules on the three membrane materials than in the control plate, with SIS membranes showing the greatest number (Figure 3), indicating that the SIS membrane possesses the greatest BMSC mineralization promoting activity.

Detection of osteogenic factor expression in vitro

We next explored the effect of different membrane materials on the expression of osteogenesis-related factors in BMSCs to assess their osteogenic abilities. We found the mRNA expression levels of *BMP-2*, *Runx2*, *ALP*, and OPN to be highest in the SIS membrane group (Figure 4a). Consistent with this pattern, their protein expression levels were also highest in the SIS membrane group (Figure 4b and c) and supported by immunofluorescence (Figure 4d). These results demonstrate that SIS membranes promote osteogenesis-related factor expression more than other membrane types.

Osteogenesis ability in vivo

Micro-CT 3D reconstructions in the skull defect model after 6 weeks showed that the defect area in the blank control group had almost no reduction, and tomography showed that the defect area was entirely in a low-density transmission area (Figure 5a). In the Heal-all and Dentium membrane groups, a small amount of new bone formation was observed around the defect, but no complete healing had been formed (Figure 5a). However, in the SIS membrane group, the range of bone defects was significantly reduced compared to the other groups (Figure 5a), and tomography showed a thin-layer image of increased bone density in the defect area (Figure 5a). In addition, BV/TV values in the SIS membrane group were significantly higher than in the other three groups (Figure 5b).

Histological staining

The infiltration of fibrous tissue and the formation of new bone was evaluated by H&E and Masson staining. There was almost no new bone formation in the blank control group, and the defect area was filled with fibrous connective tissue (Figure 6a). In contrast, a small amount of new bone tissue was present in the defect area of the three membrane groups, with homogeneous red staining and no obvious inflammatory response (Figure 6a). Notably, the amount of new bone formation was greatest in the SIS membrane group (Figure 6a). Moreover, collagen formation in the SIS

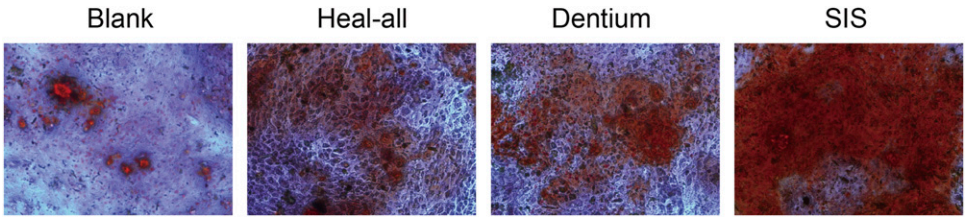

Figure 3. The calcium salt deposition of BMSCs cultured on the different membranes. Cells were stained with alizarin red after 7 days of culturing.

membrane group was more mature than that in the Heal-all and Dentium membrane groups (Figure 6b).

Discussion

In recent years, numerous studies have focused on developing asymmetric GBR membranes.[22–24] The surface morphology of the membrane affects its application in GBR. Its dense layer prevents epithelial cells and fibrous connective tissue from entering the bone defect area, and its loose layer promotes the adhesion of osteoblasts and blood clot stability to promote bone regeneration.[25] Among three membranes, the SIS membrane had an asymmetric structure that could provide sufficient time and a suitable environment for bone cell growth and enable bone tissue regeneration.

In addition, cell proliferation is the basis of new tissue formation in most systems.[26] However, we found the three membranes to have no significant effect on cell growth, indicating that they have good biocompatibility, a prerequisite for their use in hosts. The cell proliferation promoting abilities of the SIS membrane may be related to FGF, TGF, and other biologically active factors within it. Studies have found FGF and TGF to significantly promote BMSC proliferation and osteogenic differentiation through the protein kinase B (Akt1), extracellular signal-regulated kinase (Erk), and other signal pathways.[27–29]

In this study, the expression of osteogenic factors in BMSCs was explored. BMP-2, Runx2, and ALP are classic bone formation factors, and their expression is closely related to bone regeneration.[30–32] Our results showed that the SIS membrane increased the expression of BMP-2, Runx2, ALP, and OPN in BMSCs the most compared with the other membranes, indicating that the SIS membrane has a significant osteogenic effect in vitro. The 3D structure of the SIS membrane can provide a suitable microenvironment for cell proliferation, survival, and adhesion, and various growth factors contained in SIS also contribute to cell differentiation and tissue regeneration.[33] FGF plays an important role in osteogenesis and angiogenesis during bone healing and development,[34] and bFGF can induce BMSC osteogenic differentiation,[27] which is conducive to bone tissue regeneration. In addition, the continuous supply of VEGF is also important for tissue regeneration. It has been shown that the application of VEGF enhances the osteogenic effect of human osteoblast-like MG-63 cells.[35] VEGF can also synergize with BMP-2 to accelerate bone formation and maturation through the p38 protein kinase pathway.[36,37] Therefore, the SIS membrane might promote new bone formation through its multiple active components, providing greater osteogenic induction effects than other membrane materials.

Collagen regeneration and new bone formation are important processes in tissue regeneration.[38] The three membranes provide specific repair effects on bone defects, while the osteogenic effect of the SIS membrane group was better than the Heal-all and Dentium membrane groups. Their similarities might reflect that they are all collagen membranes with good biocompatibility and degradability, and their fabrication techniques retain the 3D spatial structure, providing good scaffolds for bone tissues and cells and conducive to the growth of cells and repair of bone defects.

However, the SIS membrane group had a stronger effect on repairing bone defects in vivo and in vitro than the Heal-all and Dentium membrane groups, likely due to the various growth factors and other components it contains that promote osteogenesis. Glycosaminoglycans such as chondroitin sulfate are major ECM components that play an important role in organogenesis.[39,40] Chondroitin sulfate can bind to N-cadherin and regulate osteoblast differentiation through ERK1/2, Smad3, and Smad1/5/8 signaling pathways and plays an important role in promoting osteogenesis in a variety of bone defect models.[41–43] In addition, heparin can enhance the osteogenic ability of biomaterials,[44] increasing the expression and activity of *ALP* in primary human bone marrow stromal cells (hBMSCs) and promoting mineralization during osteogenic differentiation and transformation.[45]

In conclusion, the SIS absorbable collagen membrane has high biocompatibility, prevents the invasion of fibroblasts from surrounding soft tissue, provides bone cells sufficient time to proliferate, and retains the original 3D ECM structure, providing a good scaffold for bone cell growth. SIS membrane contains glycosaminoglycan, heparin, and a variety of growth factors, which can effectively promote and accelerate bone regeneration and achieve a better osteogenic repair effect. However, further research into the effect of the SIS membrane on osteogenesis is needed and how to improve its performance in promoting

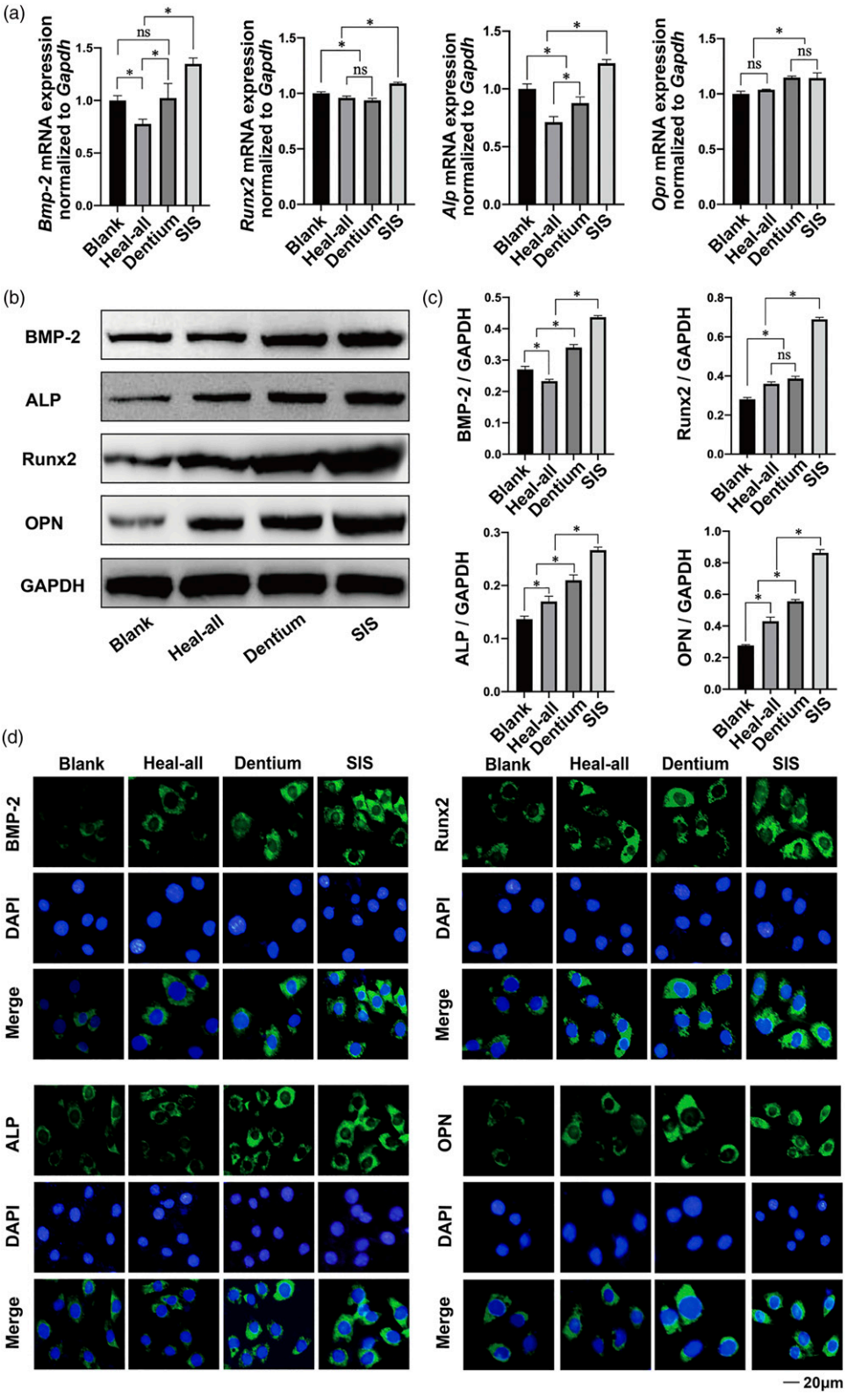

Figure 4. Effects of the SIS, Heal-all, and Dentium membranes on osteogenesis-related factors *BMP-2*, *Runx2*, *ALP*, and *OPN* in BMSCs. (a) mRNA expression. (b) Protein expression. (c) Quantitative analysis of Western blots. (d) Representative confocal microscopic images after staining, where the factors are shown in green and cell nuclei in blue. In parts a and c, *denotes $p < 0.05$.

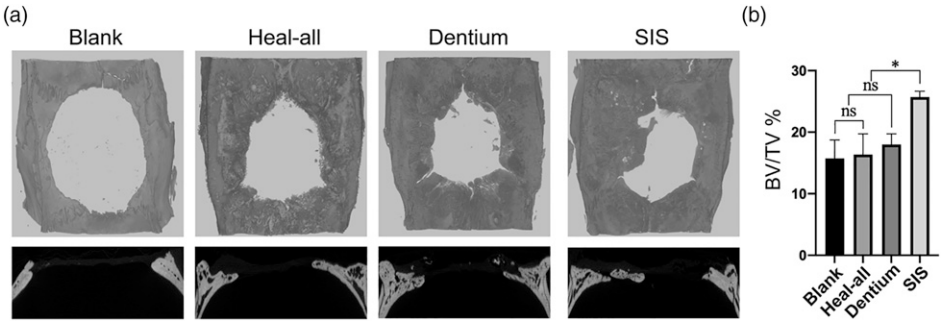

Figure 5. Evaluation of in vivo osteogenesis ability. (a) Representative 3D reconstruction and sagittal surface images of rat calvarial defects covered with each membrane. (b) BV/TV values in each group (*denotes $p < 0.05$).

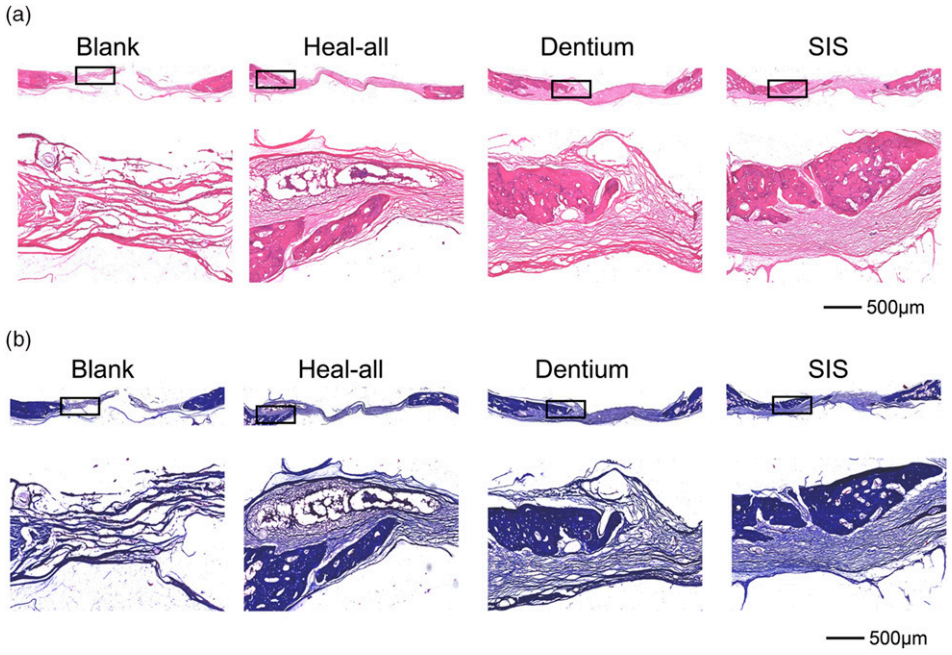

Figure 6. Histological analysis 6 weeks post-transplantation. (a) H&E staining. (b) Masson trichrome staining.

bone and reducing regeneration time. In addition, the scaffold degradation rate is also a key factor in tissue remodeling.[46] The study found that the SIS membrane rapidly degraded, which is unfavorable for maintaining the mechanical and supporting properties of the scaffold.[47] If the degradation and mechanical properties of the SIS membrane can be improved by modification, its application effects will also improve. Nevertheless, the SIS membrane shows great practical potential in GBR.

Conclusion

In this study, the GBR potential of the SIS membrane was evaluated. The results show that the SIS membrane has an asymmetric structure and good biocompatibility, provides a microenvironment suitable for inducing BMSC osteogenic differentiation, and promotes the expression of important osteogenic-related factors. In addition, the SIS membrane performed well in promoting early bone formation in the rat calvarial defect model. The SIS membrane has great potential as a new type of GBR membrane.

Declaration of Conflicting Interests

The author(s) declared no potential conflicts of interest with respect to the research, authorship, and/or publication of this article.

Funding

The author(s) disclosed receipt of the following financial support for the research, authorship, and/or publication of this article: This work is supported by the National Natural Science Foundation of China (NSFC; Grant No. 81701019), the Clinical Research Special

Fund of Wu Jieping Medical Foundation (320.6750.2021-07-21), the Guangdong Basic and Applied Basic Research Foundation (No. 2020A1515111182), the Scientific Foundation of Tianjin Education Commission (Grant No. 2019KJ173) and the Science and technology project of Tianjin Health Committee (Grant No. QN20026).

ORCID iD

Zihao Liu https://orcid.org/0000-0003-4878-1275

References

1. Nauth A, Schemitsch E, Norris B, et al. Critical-size bone defects: is there a consensus for diagnosis and treatment? *J Orthop Trauma* 2018; 32(Suppl 1): S7–S11.
2. Boda SK, Almoshari Y, Wang H, et al. Mineralized nanofiber segments coupled with calcium-binding BMP-2 peptides for alveolar bone regeneration. *Acta Biomater* 2019; 85: 282–293.
3. Khojasteh A, Kheiri L, Motamedian SR, et al. Guided bone regeneration for the reconstruction of alveolar bone defects. *Ann Maxillofac Surg* 2017; 7(2): 263–277.
4. Dimitriou R, Jones E, McGonagle D, et al. Bone regeneration: current concepts and future directions. *BMC Med* 2011; 9: 66.
5. Sheikh Z, Qureshi J, Alshahrani AM, et al. Collagen based barrier membranes for periodontal guided bone regeneration applications. *Odontology* 2017; 105(1): 1–12.
6. Retzepi M and Donos N. Guided bone regeneration: biological principle and therapeutic applications. *Clin Oral Implants Res* 2010; 21(6): 567–576.
7. Hardwick R, Hayes BK, Flynn C, et al. Devices for dentoalveolar regeneration: an up-to-date literature review. *J Periodontol* 1995; 66(6): 495–505.
8. Song JH, Kim HE, Kim HW, et al. Collagen-apatite nanocomposite membranes for guided bone regeneration. *J Biomed Mater Res B Appl Biomater* 2007; 83(1): 248–257.
9. Soldatos NK, Stylianou P, Koidou VP, et al. Limitations and options using resorbable versus nonresorbable membranes for successful guided bone regeneration. *Quintessence Int* 2017; 48(2): 131–147.
10. Maleki Dizaj S, Sharifi S, Jahangiri A, et al. Electrospun nanofibers as versatile platform in antimicrobial delivery: current state and perspectives. *Pharm Dev Technol* 2019; 24(10): 1187–1199.
11. Lee SW and Kim SG. Membranes for the guided bone regeneration. *Maxillofac Plast Reconstr Surg* 2014; 36(6): 239–246.
12. Mansour A, Mezour MA, Badran Z, et al. *Extracellular matrices for bone regeneration: a literature review. *Tissue Eng A* 2017; 23(23–24): 1436–1451.
13. Cunniffe GM, Díaz-Payno PJ, Sheehy EJ, et al. Tissue-specific extracellular matrix scaffolds for the regeneration of spatially complex musculoskeletal tissues. *Biomaterials* 2019; 188: 63–73.
14. Gattazzo F, Urciuolo A, Bonaldo P, et al. Extracellular matrix: a dynamic microenvironment for stem cell niche. *Biochim Biophys Acta* 2014; 1840(8): 2506–2519.
15. Janis AD, Johnson CC, Ernst DM, et al. Structural characteristics of small intestinal submucosa constructs dictate in vivo incorporation and angiogenic response. *J Biomater Appl* 2012; 26(8): 1013–1033.
16. Ji Y, Zhou J, Sun T, et al. Diverse preparation methods for small intestinal submucosa (SIS): decellularization, components, and structure. *J Biomed Mater Res A* 2019; 107(3): 689–697.
17. Voytik-Harbin SL, Brightman AO, Kraine MR, et al. Identification of extractable growth factors from small intestinal submucosa. *J Cel Biochem* 1997; 67(4): 478–491.
18. Kim K and Kim MS. An injectable hydrogel derived from small intestine submucosa as a stem cell carrier. *J Biomed Mater Res B Appl Biomater* 2016; 104(8): 1544–1550.
19. Kim KS, Lee JY, Kang YM, et al. Small intestine submucosa sponge for in vivo support of tissue-engineered bone formation in the presence of rat bone marrow stem cells. *Biomaterials* 2010; 31(6): 1104–1113.
20. Wang F, Song Q, Du L, et al. Development and characterization of an acellular porcine small intestine submucosa scaffold for use in corneal epithelium tissue engineering. *Curr Eye Res* 2020; 45(2): 134–143.
21. Shohara R, Yamamoto A, Takikawa S, et al. Mesenchymal stromal cells of human umbilical cord Wharton's jelly accelerate wound healing by paracrine mechanisms. *Cytotherapy* 2012; 14(10): 1171–1181.
22. Ghavimi MA, Bani Shahabadi A, Jarolmasjed S, et al. Nanofibrous asymmetric collagen/curcumin membrane containing aspirin-loaded PLGA nanoparticles for guided bone regeneration. *Sci Rep* 2020; 10(1): 18200.
23. Fidalgo C, Rodrigues MA, Peixoto T, et al. Development of asymmetric resorbable membranes for guided bone and surrounding tissue regeneration. *J Biomed Mater Res A* 2018; 106(8): 2141–2150.
24. Kim HY, Park JH, Byun JH, et al. BMP-2-immobilized porous matrix with leaf-stacked structure as a bioactive GBR membrane. *ACS Appl Mater Inter* 2018; 10(36): 30115–30124.
25. Ma S, Adayi A, Liu Z, et al. Asymmetric collagen/chitosan membrane containing minocycline-loaded chitosan nanoparticles for guided bone regeneration. *Sci Rep* 2016; 6: 31822.
26. Wang W, Zhang X, Chao NN, et al. Preparation and characterization of pro-angiogenic gel derived from small intestinal submucosa. *Acta Biomater* 2016; 29: 135–148.
27. Ricci L and Srivastava M. Wound-induced cell proliferation during animal regeneration. *Wiley Interdiscip Rev Dev Biol* 2018; 7(5): e321.
28. Du M, Zhu T, Duan X, et al. Acellular dermal matrix loading with bFGF achieves similar acceleration of bone regeneration to BMP-2 via differential effects on recruitment, proliferation

and sustained osteodifferentiation of mesenchymal stem cells. *Mater Sci Eng C Mater Biol Appl* 2017; 70(Pt 1): 62–70.
29. Li J, Ge L, Zhao Y, et al. TGF-β2 and TGF-β1 differentially regulate the odontogenic and osteogenic differentiation of mesenchymal stem cells. *Arch Oral Biol* 2022; 135: 105357.
30. Li P, Deng Q, Liu J, et al. Roles for HB-EGF in mesenchymal stromal cell proliferation and differentiation during skeletal growth. *J Bone Miner Res* 2019; 34(2): 295–309.
31. Betz VM, Ren B, Messmer C, et al. Bone morphogenetic protein-2 is a stronger inducer of osteogenesis within muscle tissue than heterodimeric bone morphogenetic protein-2/6 and -2/7: implications for expedited gene-enhanced bone repair. *J Gene Med* 2018; 20(9): e3042.
32. Agas D, Sabbieti MG, Marchetti L, et al. FGF-2 enhances Runx-2/smads nuclear localization in BMP-2 canonical signaling in osteoblasts. *J Cel Physiol* 2013; 228(11): 2149–2158.
33. Cao G, Huang Y, Li K, et al. Small intestinal submucosa: superiority, limitations and solutions, and its potential to address bottlenecks in tissue repair. *J Mater Chem B* 2019; 7(33): 5038–5055.
34. Qu D, Li J, Li Y, et al. Angiogenesis and osteogenesis enhanced by bFGF ex vivo gene therapy for bone tissue engineering in reconstruction of calvarial defects. *J Biomed Mater Res A* 2011; 96(3): 543–551.
35. Rumney RMH, Lanham SA, Kanczler JM, et al. In vivo delivery of VEGF RNA and protein to increase osteogenesis and intraosseous angiogenesis. *Sci Rep* 2019; 9(1): 17745.
36. Wang T, Guo S, Zhang H, et al. Synergistic effects of controlled-released BMP-2 and VEGF from nHAC/PLGAs scaffold on osteogenesis. *Biomed Res Int* 2018; 2018: 3516463.
37. Sharmin F, O'Sullivan M, Malinowski S, et al. Large scale segmental bone defect healing through the combined delivery of VEGF and BMP-2 from biofunctionalized cortical allografts. *J Biomed Mater Res B Appl Biomater* 2019; 107(4): 1002–1010.
38. Wang D, Ji ZL, Wang JM, et al. Tenogenic differentiation of mesenchymal stem cells improves healing of linea alba incision. *Int J Abdom Wall Hernia Surg* 2018; 1: 13–18.
39. Förster Y, Bernhardt R, Hintze V, et al. Collagen/glycosaminoglycan coatings enhance new bone formation in a critical size bone defect-a pilot study in rats. *Mater Sci Eng C Mater Biol Appl* 2017; 71: 84–92.
40. Ida-Yonemochi H, Morita W, Sugiura N, et al. Craniofacial abnormality with skeletal dysplasia in mice lacking chondroitin sulfate N-acetylgalactosaminyltransferase-1. *Sci Rep* 2018; 8(1): 17134.
41. Koike T, Izumikawa T, Tamura J, et al. Chondroitin sulfate-E fine-tunes osteoblast differentiation via ERK1/2, Smad3 and Smad1/5/8 signaling by binding to N-cadherin and cadherin-11. *Biochem Biophys Res Commun* 2012; 420(3): 523–529.
42. Andrews S, Cheng A, Stevens H, et al. Chondroitin sulfate glycosaminoglycan scaffolds for cell and recombinant protein-based bone regeneration. *Stem Cell Transl Med* 2019; 8(6): 575–585.
43. Li Y, Wu J, Jiang J, et al. Chondroitin sulfate-immobilized polyethylene terephthalate with extracellular matrix-mimetic immunoregulatory function for osseointegration. *J Mater Chem* 2019; 7: 223–246.
44. Takeda Y, Honda Y, Kakinoki S, et al. Surface modification of porous alpha-tricalcium phosphate granules with heparin enhanced their early osteogenic capability in a rat calvarial defect model. *Dent Mater J* 2018; 37(4): 575–581.
45. Simann M, Schneider V, Le Blanc S, et al. Heparin affects human bone marrow stromal cell fate: promoting osteogenic and reducing adipogenic differentiation and conversion. *Bone* 2015; 78: 102–113.
46. Tharappel J, Wennergren JE, Lee EY, et al. A comparative analysis of ventral hernia repair with a porcine hepatic-derived matrix and porcine dermal matrix. *Int J Abdom Wall Hernia Surg* 2019; 2: 89–95.
47. Bi X, Li L, Mao Z, et al. The effects of silk layer-by-layer surface modification on the mechanical and structural retention of extracellular matrix scaffolds. *Biomater Sci* 2020; 8(14): 4026–4038.